RSC Publishing Faraday Discussions

Probing eumelanin photoprotection using a catechol:quinone heterodimer model system

Journal:	*Faraday Discussions*
Manuscript ID	FD-ART-12-2018-000231.R1
Article Type:	Paper
Date Submitted by the Author:	07-Jan-2019
Complete List of Authors:	Grieco, Christopher; Ohio State University, Chemistry and Biochemistry Empey, Jennifer; Ohio State University, Chemistry and Biochemistry Kohl, Forrest; Ohio State University, Chemistry and Biochemistry Kohler, Bern; Ohio State University, Chemistry and Biochemistry

Probing eumelanin photoprotection using a catechol:quinone heterodimer model system

Christopher Grieco, Jennifer M. Empey, Forrest R. Kohl, Bern Kohler*

Department of Chemistry and Biochemistry, The Ohio State University, 100 West 18th Avenue, Columbus, Ohio 43210, United States

*Corresponding author

Abstract

Eumelanin is a natural pigment with photoprotective and radical scavenging characteristics that are vital for a multitude of living organisms. However, the molecular mechanisms behind these functions remain obscure, in part because eumelanin is a heterogeneous polymer composed of a complex assortment of structural and chemical domains. Despite uncertainty about its precise structure, the functional units of eumelanin are thought to include quinones in various oxidation states. Here, we investigate the photochemistry of a catechol:*o*-quinone heterodimer as a model system for uncovering the photoprotective roots of eumelanin. Ultrafast transient absorption measurements in the UV to near-IR spectral regions are used to identify the photochemical processes that follow selective excitation of the *o*-quinone in the heterodimer using 395 nm light. We find that both singlet and triplet *o*-quinone excited states induce hydrogen atom transfer from the catechol, forming semiquinone radical pairs that persist beyond 2.5 ns, the upper time limit accessible by our instrument. Furthermore, the hydrogen atom transfer reaction was found to occur 1000 times faster via the singlet channel. Excited state pathways such as these may be important in eumelanin where similar hydrogen-bonded interfaces are believed to exist between catechol and *o*-quinone functional groups.

1. Introduction

Eumelanin is a redox-mutable biopolymer with photoprotective and radical scavenging character that is widely distributed throughout nature.[1, 2] However, its excited state deactivation processes are not well understood due to the heterogeneity of its physical and chemical structure, which may give rise to a number of different deactivation pathways. Studies of model systems containing substructures proposed to occur in eumelanin have led to important insights, but much of this work has focused on intramolecular processes that occur within monomers and oligomers of 5,6-dihydroxyindole (DHI) and 5,6-dihydroxyindole carboxylic acid (DHICA), or intermolecular processes with the solvent (see Scheme 1).[3-7] Very little is known about how intermolecular interactions between DHI and/or DHICA units in different redox states affect excited state relaxation processes in eumelanin.[8]

Two major functional groups present in eumelanin, *ortho*-positioned dihydroxy (catechol) and quinone groups, are believed to interact through π-stacking and/or intermolecular hydrogen bonding.[9-11] Because the indole units present in eumelanin bearing these groups spontaneously polymerize in solution to form eumelanin, we consider the chemically stable 3,5-di-*tert*-butyl-substituted catechol (C) and *o*-quinone (Q) molecules as an alternative model system. To our knowledge, only one account[12] attempts to time-resolve the photochemistry of heterodimers of this pair. Using nanosecond transient absorption spectroscopy, Van Anh et al.[12] determined that a semiquinone radical pair is produced upon selective photoexcitation of Q. The authors concluded that this species must be a neutral radical pair formed by proton-coupled electron transfer, and not a radical ion pair formed by electron transfer, based on a 20 nm shift in the transient absorption band. However, the mechanism for radical pair formation could not be time-resolved with their instrumentation, and additional spectral support for this assignment is desirable.

In this work, we expand on the results of Van Anh et al.[12] by time-resolving the dynamics immediately following selective excitation of the quinone in hydrogen-bonded heterodimers of Q and C in cyclohexane. Our results support their assignment of neutral radical pair formation, and reveal the complex excited state pathways that precede formation of this species. In particular, the singlet excited state of Q may either induce hydrogen atom transfer from C to form a semiquinone neutral radical pair, or undergo ultrafast intersystem crossing. This bifurcated deactivation process is controlled by the hydrogen bond joining Q and C. The triplet state of Q also drives hydrogen atom transfer from C to form a triplet semiquinone neutral radical pair, but on a much slower timescale. Our results reveal a hydrogen atom transfer interface that serves as a light-driven radical generation center that may be present in eumelanin.

2. Methods

2.1. Materials and solution preparation

All chemicals were purchased and used as received. Cyclohexane was from Acros Organics (HPLC grade, 99.8%), and 2-propanol was from Sigma Aldrich (ACS reagent grade, >99.5%). The 3,5-di-*t*-butylcatechol (C) and 3,5-di-*t*-butyl-*o*-quinone (Q) were from Sigma Aldrich (98% purity each). For UV/Vis and FTIR spectroscopy measurements, cyclohexane solutions of Q and C were prepared in concentrations ranging from 5–100 mM. To prepare heterodimer solutions, Q and C were dissolved in cyclohexane to yield equal initial concentrations (1:1 mole ratio). Hereafter, the concentration of every Q+C solution mentioned in the text refers to the initial concentration of Q, which is equal to the initial concentration of C. Steady-state spectroscopy measurements were performed on Q+C solutions with concentrations ranging from 5–100 mM. For femtosecond transient absorption measurements, solutions of Q, C, and Q+C were all 30 mM. Additional measurements were performed with 2-propanol.

2.2. UV/Vis spectroscopy

UV/Vis spectra of all samples were recorded using a Cary 5000 UV/Vis/NIR Spectrometer (Agilent; Santa Clara, CA). Solutions were measured in a custom-made demountable liquid cell with Teflon spacers and CaF_2 windows. The pathlengths used ranged from 25–500 μm depending on the sample concentration in order to keep the maximum absorbance above 300 nm below 1.0. The spectral resolution was 0.25 nm.

2.3. FTIR Spectroscopy

Vibrational spectroscopy was performed using a FTIR spectrometer (FT/IR-4200, JASCO; Easton, MD). All samples were measured in the same liquid cell used for UV/Vis spectroscopy, but with a pathlength of 100 μm for solutions containing monomer concentrations exceeding 50 mM, and 200 μm for all other samples. The spectral resolution was 0.5 cm^{-1}.

2.4. Femtosecond UV/Vis and Vis/NIR Pump-Probe spectroscopy

Femtosecond UV/Visible measurements were performed using an ultrafast UV/Vis pump-probe spectrometer described previously.[8] For all experiments, the excitation wavelength was 395 nm, and the incident laser fluence calculated assuming Gaussian spatial and temporal profiles was approximately 500 μJ/cm^2. For each sample scan, about 4 mL of solution was recirculated through a demountable liquid flow cell (TFC-M25-3, Harrick Scientific Products; Pleasantville, NY) with CaF_2 windows and a 500 μm Teflon spacer. The absorbance of each sample at 395 nm was approximately 0.6. A prism spectrometer was used to disperse the probe light after the sample on a Si CCD detector, and the detected spectral range was 320–630 nm.

Probe pulses for femtosecond visible/near-infrared (Vis/NIR) broadband measurements between 600 and 1100 nm were obtained from a white light supercontinuum that was generated by focusing 1400 nm pulses in a 5 mm thick sapphire

window. The 1400 nm pulses were from the signal field produced by driving an optical parametric amplifier (TOPAS Prime, Coherent; Santa Clara, CA) using a portion of the output of a ~100 fs Ti:Sapphire laser amplifier (Astrella, Coherent; Santa Clara, CA). Measurements carried out on cyclohexane solutions were conducted using the same Si CCD detector used in the femtosecond UV/Visible broadband experiments. The measurements on the 2-propanol solution were carried out using an InGaAs array detector, an upgrade to our NIR detection system that was completed during the course of these experiments.

The total transient absorption spectra between 320 nm and 1100 nm were measured piecewise using the femtosecond UV/Vis and Vis/NIR spectrometers. To connect the spectra, a single scaling factor was applied to the entire Vis/NIR dataset until the mean square deviations in signal intensities for both the UV/Vis and Vis/NIR datasets were minimized. This correction factor, which never exceeded a value of 1.315, accounts for slight differences in excitation fluence used between each set of measurements. After scaling, the signals measured in the region of overlap between 600 nm and 630 nm were averaged. The connected transient absorption spectra were modeled with target analysis using the Glotaran software package (version 1.5.1).[13]

3. Results

The FTIR spectra of a series of equimolar Q+C solutions in cyclohexane (Fig. 1a) change dramatically with concentration. This is easily seen when the spectra are presented as the apparent molar absorption coefficient, $\varepsilon_{apparent}$, which is defined as the measured absorbance divided by the product of the initial concentration of Q (or C) and the sample pathlength. For the 5 mM Q+C solution (black trace in Fig, 1a), two intense and narrow peaks appear at 3561 cm^{-1} and 3626 cm^{-1} due to O-H stretching by C (see the FTIR spectra of the separate Q and C solutions in Fig. S1). A broader, lower-frequency O-H stretching peak is also observed at 3460 cm^{-1}, which is assigned to the heterodimer formed between Q and C (hereafter designated by Q:C). As the concentration increases, the two sharp peaks decrease while the 3460 cm^{-1} peak increases and a new narrow peak grows in at 3540 cm^{-1}. These spectra were decomposed to obtain the Q:C heterodimer FTIR spectrum, which is compared to the measured Q and C monomer spectra in Fig. 1b. The Q:C heterodimer spectrum lacks the 3626 cm^{-1} band of the C monomer. In addition to a broad band at 3460 cm^{-1}, the heterodimer has a narrow band at 3540 cm^{-1} that is red shifted compared to the 3561 cm^{-1} band of C. These spectra, which will be discussed below in detail, were used to deduce the hydrogen bonded structures shown in Fig. 1c.

[insert Figure 1]

Fig. 2a shows the UV/Vis spectra recorded for cyclohexane solutions of Q, C, and Q+C. Each solution has the same concentration used in the femtosecond transient absorption experiments. The π→π* transition of Q appears at 386 nm and 393 nm for the Q and Q+C solutions, respectively. UV/Vis spectra recorded in a sufficiently wide spectral window to see the weak n→π* transition of Q at approximately 595 nm are shown in Fig. S3. Assignment of the n→π* transition is supported by the observed blue shifting of this band as the solvent polarity is increased (Fig. S5 and S6). UV/Vis spectra of Q+C solutions varying between 5 mM and 100 mM are shown in Fig. S7 along with difference spectra. Based on the FTIR spectra of the 30 mM solutions, the UV/Vis spectrum of the equimolar Q+C solution is decomposed to reveal the contributions of the Q monomers, C monomers, and Q:C heterodimers in Fig. 2b. The contributions to the total absorption at 395 nm by the populations of the Q monomer and the Q:C heterodimer are used later to isolate their individual transient absorption spectra.

[insert Figure 2]

Transient absorption spectra were recorded for Q and Q+C solutions in cyclohexane (Fig. 3) using a pump wavelength of 395 nm to excite the π→π* band of Q. The transient spectra for the Q+C solution in Fig. 3 have been corrected by subtracting signal contributions from the Q monomer as discussed in the ESI. The raw, uncorrected transient spectrum for the Q+C solution is shown in Fig. S11. The 2D maps in Figs. 3a and 3b are plotted on a linear photon energy scale, while the spectral slices in Figs. 3c and 3d are graphed on a linear wavelength axis. For both Q monomers and Q:C heterodimers, intense photoinduced absorptions (PIAs) are observed at the UV wavelengths for all time delays, while weaker PIAs are observed at the visible wavelengths. A negative signal assigned to a ground state bleach (GSB) feature is observed in the vicinity of the π→π* peak of the electronic ground state (see inverted ground state absorption spectra, as indicated by the gray curves in Figs. 3c and 3d).

[insert Figure 3]

The 0.5 ps spectrum of the Q monomer (Fig. 3c) has a broad peak at 580 nm, a shoulder at 462 nm, and an additional broad peak around 1100 nm (see Fig. S15 for an extended spectrum). As discussed later, these peaks can be identified with electronic transitions predicted from UV/Vis spectroscopy, which are included in Fig. 3c. Over time, the transient spectrum evolves into a narrower band with clear vibronic structure centered at approximately 533 nm (see dark blue curve). The 0.5 ps

spectrum of the Q:C heterodimer (Fig. 3d) somewhat resembles that of the Q monomer. However, it possesses a peak at approximately 610 nm that lacks the shoulder seen in the Q monomer at 462 nm, and has a significantly broadened tail extending into the NIR region. After several picoseconds, this spectrum evolves into one with peaks at approximately 550 nm and 710 nm. By 2 ns, the peak at 550 nm has completely decayed, while the peak at 710 nm continues to grow in intensity and a distinct and narrow peak is seen at 370 nm (see red arrow in Fig. 3d).

The early-time transient absorption spectrum of the Q:C heterodimer averaged from 300 to 700 fs is presented in Fig. 4a and Fig. 4b. This spectrum differs from the transient spectra recorded for the Q monomer in cyclohexane and the hydrogen-bonding solvent, 2-propanol (Fig. 4a). Target analysis of the Q:C heterodimer spectrum in Fig. 3b reveals that additional absorbing species contribute to the early spectrum of the Q:C heterodimer (Fig. 4b). One of these species produces a peak at 710 nm (pink curve in Fig. 4b), which matches the peak position seen in the 2000 ps spectrum in Fig. 3d. Fig. 4d compares the species associated difference spectrum (SADS) of this species, SADS 2, to that of the longest-lived species, SADS 4. The two spectra share a peak location of 710 nm, but SADS 4 appears narrower. This reflects the dynamic peak narrowing observed in the transient absorption spectrum of the Q:C heterodimer (Fig. 4c).

[insert Figure 4]

Transient absorption kinetics for the Q monomer and the Q:C heterodimer are compared in Fig. 5. The kinetics were obtained by averaging the transient spectra in Fig. 3 over the indicated wavelength ranges, which were selected to correspond to peaks in the transient spectra highlighted above. For Q monomers (Fig. 5a), the kinetic signals averaged over 650–1100 nm decay within ~25 ps, but include a component that extends beyond 2 ns. The kinetics averaged over 475–580 nm exhibit a rapid decay over the first few picoseconds, followed by a slower growth in intensity over the first ~25 ps. This signal does not decay by 2 ns.

For the Q:C heterodimer (Fig. 5b), the kinetic signal averaged over 950–1100 nm exhibits a faster initial decay than the 650–1100 nm trace for Q monomers, followed by a slower decay during the first 25 ps. The kinetics averaged over 500–530 nm exhibit a fast decay during the first few picoseconds followed by a slower growth over the next several picoseconds. Unlike the 475–580 nm trace for Q monomers, the 500–530 nm trace for Q:C heterodimers decays completely by 2 ns. The kinetics averaged over 650–800 nm contain a rapid decay component like the 950–1100 nm trace. However, the signal does not decay further beyond 5 ps, but instead persists until 25 ps, after which it slowly grows during the remainder of the measured time window. This growth mirrors the decay of the 500–530 nm trace.

[insert Figure 5]

Fig. 5c shows the kinetics averaged over 415–425 nm for Q monomers and Q:C heterodimers in cyclohexane. These signals contain overlapping PIA signals that partially obscure the pure bleaching kinetics. In both systems, the intensity of the GSB traces increases in magnitude over the first few picoseconds, mirroring the decay of the 650–1100 (black squares in Fig. 5a) and 950–1100 nm (black squares in Fig. 5b) traces for the Q monomers and Q:C heterodimers, respectively, but then remain constant over the next 100 ps. Thereafter, the GSB trace for the Q monomer decays very slightly toward zero, while that for the Q:C heterodimer becomes more negative, mirroring the late growth of the 650–800 nm trace in Fig. 5b.

4. Discussion

4.1. Heterodimer formation

Intermolecular hydrogen bonding drives the association of the Q and C molecules in concentrated cyclohexane solutions. We chose the weakly-perturbing solvent, cyclohexane, to isolate the interaction between Q and C from interactions of each with the solvent. Structural sensitivity of the O-H stretching modes in hydrogen-bonded systems makes vibrational spectroscopy a useful method for characterizing their structure.[8, 14, 15] As such, FTIR spectroscopy of the O-H stretching modes in C can be used to characterize the hydrogen bonding structure of Q:C heterodimers that form in Q+C mixture solutions.

The sharp O-H stretching peaks at 3561 cm^{-1} and 3626 cm^{-1} in Fig. 1a were previously assigned to the intramolecularly hydrogen bonded (b) and free (f) O-H groups of the C monomer (see left structure in Fig. 1c).[8, 14, 15] Indeed, these peaks are present for C solutions ranging in concentration from 5 mM to 100 mM (Fig. S1a). The redshifted and broadened peak at 3460 cm^{-1} is not present in the C-only solution and must originate from intermolecular hydrogen bonding between Q and C molecules. The growth of this peak with increasing Q and C concentration is associated with the appearance of the new narrow peak at 3540 cm^{-1} (peak b' in Fig. 1a). This spectral behavior has been previously observed in solutions of catechol in aprotic solvents containing hydrogen bond-accepting bases.[15] Similar observations have been made for 3,5-di-*t*-butylcatechol.[14] In these studies, the catechol molecule forms complexes with base molecules through intermolecular hydrogen bonding with the free O-H group. This complexation causes the intensity of the f band to decrease and is accompanied by the growth of a broader, downshifted band below 3500 cm^{-1} due to the intermolecular hydrogen bond. The intermolecular hydrogen bond causes the intramolecular hydrogen bond in catechol to strengthen via cooperativity,[14, 15] inducing the b band to change into

the lower frequency b' band. Based on this work, we conclude that a similar complexation mechanism occurs between the C and Q molecules in the heterodimer, as illustrated in Fig. 1c. In particular, one O-H group in C donates a hydrogen bond to Q, while the other remains intramolecularly hydrogen bonded.

The magnitude of the frequency shift of the b band of catechol and its derivatives is well correlated with the strength of the intermolecular hydrogen bond, or proton acceptor ability of the base.[14, 15] In particular, Varfolomeev et al. have demonstrated that this shift[15] is linearly correlated to the hydrogen bond formation enthalpy of methanol with proton acceptors.[16] Using this correlation, the 21 cm^{-1} downshift of the b band in Fig. 1 indicates a hydrogen bond formation enthalpy between C and Q of approximately -13.3 kJ mol^{-1}, most similar to that for the catechol:dimethylsulfoxide complex.[15] Bifurcation of the hydrogen bond, which would produce a 3-centered interaction between the O-H group in C and the C=O groups in Q, is unlikely because the resulting 5-membered ring structure would possess an angular geometry (120°) unfavorable to hydrogen bond formation.[17] We therefore conclude that the free O-H group in C hydrogen bonds to only one of the C=O groups in Q.

The concentration of Q:C heterodimers in the Q+C solutions was quantified as a first step toward interpreting the transient absorption spectra, assuming a simple equilibrium model:

$$\mathrm{Q} + \mathrm{C} \leftrightarrow \mathrm{Q{:}C} \qquad K_{eq} = 91\ M^{-1} \tag{1}$$

From the FTIR spectra, the concentration of C monomers, [C] can be determined from the decrease in extinction of the free O-H peak at 3626 cm^{-1} (see the ESI for further details).[8] The concentration of the Q:C heterodimers, [Q:C], can be determined by subtracting [C] from the initial C concentration, $[C]_{init}$:

$$[\mathrm{Q{:}C}] = [\mathrm{C}]_{\mathrm{init}} - [\mathrm{C}] \tag{2}$$

Using eq. 2, the concentration of Q:C heterodimers in the 30 mM Q+C solution used in the ultrafast spectroscopy measurements was determined to be 17 mM. Using eqs. 1 and 2, the equilibrium constant, K_{eq}, for the dimerization reaction was estimated to be 91 M^{-1}. Additionally, the molar absorption spectrum of the Q:C heterodimer could be determined (Fig. 1b).

4.2. UV/Vis spectroscopy and discriminating the transient absorption spectra produced by monomers and heterodimers

The UV/Vis spectra in Fig. 2a are dominated at wavelengths longer than 300 nm by the π→π* transition of Q, which is assigned based on the magnitude of the molar extinction coefficient (2100 M^{-1} cm^{-1}) and previous reports.[18-20] The n→π* transition is located at 595 nm and has a molar extinction coefficient of approximately 40 M^{-1} cm^{-1} (Fig. S3b). The redshift observed for Q+C mixtures (see Fig. 2a and Fig. S7) reflects the change in environmental polarity experienced by Q upon hydrogen bonding with C. Indeed, such a redshift of the π→π* peak (and simultaneous blueshift of the n→π* peak) of Q originates from solvatochromism (see Fig. S5) as reported previously by Van Anh et al.[12] In fact, we find that the π→π* and n→π* peak

positions correlate linearly with the Gutmann acceptor number of the solvent (Fig. S6). Ravi Kumar et al. reported a similar phenomenon for such transitions in benzophenone solutions.[21]

Based on these observations, the gradual redshift of the π→π* peak observed for the Q+C mixtures as their concentrations are increased (Fig. S7) could be explained by a gradual change in the polarity experienced by the Q molecules. However, we find that a two-state model better describes the gradual redshift of the Q+C mixtures, in which the total measured absorbance of Q+C (A_{Q+C}) can be described as the sum of the Q monomer spectrum (A_Q) and the Q:C heterodimer spectrum ($A_{Q:C}$) for all solution concentrations:

$$A_{Q+C} = A_Q + A_{Q:C} \quad (3)$$

The hydrogen bond in the Q:C heterodimer is expected to redshift its absorbance to a distinct position due to solvatochromism (Fig. S5), which would produce the gradual redshift observed as the Q population converts to Q:C (Fig. S7a). The results published in the supporting information section of Van Anh et al. show that the difference absorption spectrum of Q does not shift as the mole ratio of Q:C is increased from 1:10 to 1:80 in methylcyclohexane.[12] Likewise, we observe no significant shifting in difference spectra as the total concentration in an equimolar mixture of Q+C is increased to 100 mM (Fig. S7b). These observations support the two-state model. Notably, the redshift of the π→π* peak upon increasing solution concentration (Fig. S7a) approaches that of dilute solutions of covalently tethered Q and C molecules, which is located at 400 nm.[12]

As Fig. 2b indicates, the 395 nm excitation wavelength used in the transient absorption measurements excites both Q monomers and Q:C heterodimers present in the Q+C solution. Because the total absorption spectrum can be described using the 2-state model (eq. 3), we can decompose the transient absorption signal for the Q+C mixture, $\Delta A_{Q+C}(t)$, into components due to the Q monomers and Q:C heterodimers (see ESI section S.3 for full details),

$$\Delta A_{Q+C}(t) = \Delta A_{Q:C}(t) + \Delta A_Q(t), \quad (4)$$

where $\Delta A_{Q:C}(t)$ and $\Delta A_Q(t)$ are the transient absorption signals produced by the population of Q:C heterodimers and Q monomers, respectively. Knowledge of the absorbance fraction of each species excited allows the interfering transient absorption produced by Q monomers to be subtracted from the total measured spectrum (ΔA_{Q+C}). This is because in a mixture the TA signal of each component contributes in proportion to the ratio of the absorbance of that species to the total absorbance at the pump wavelength (see ESI). In eq. 4, cross terms describing signals arising from interactions among the various species excited are not needed because bimolecular encounters occur beyond the time window measured by our instrument (2.5 ns). For example, diffusion-limited reactions occur in cyclohexane at a rate of 7.1 x 10^9 M^{-1} s^{-1}, implying that a bimolecular encounter requires approximately 240 ns for a solute concentration of 60 mM.

The absorption spectrum of the Q+C mixture solution can be decomposed using the fraction of Q:C heterodimers determined from FTIR spectroscopy of the same solution (Fig. 2b). As a check on the accuracy of the decomposition procedure, the Q:C heterodimer peak appears at ~400 nm (Fig. 2b) in excellent agreement with the peak location of covalently tethered Q and C molecules.[12] The absorption intensities of the decomposed Q monomer and Q:C heterodimer bands at 395 nm are then used to determine how much of the Q monomer transient absorption spectrum to subtract from the total measured transient absorption spectrum of the Q+C mixture. Further details on this subtraction procedure are provided in the ESI. The results of this process are shown in Fig. 3b and Fig. 3d and will be discussed below.

4.3. Excited state dynamics of the Q monomer

Understanding of the photophysics of the Q monomer in cyclohexane is needed to interpret the results for the Q:C heterodimer. The 0.5 ps spectrum in Fig. 3c is assigned to an excited singlet state of Q (^{1}Q*) based on previous observations for other quinones.[22] Additionally, the peaks at 580 nm and 1100 nm can be assigned to the n→π* and π→n transitions of the ^{1}nπ* state of Q, respectively, as predicted from UV/Vis spectroscopy (see energy level diagram in Fig. 3c and Fig. S15). As in other quinones,[22] xanthones,[23] and benzophenone,[24] the excited singlet state undergoes ultrafast intersystem crossing in several picoseconds to yield a distinctive, blue-shifted triplet absorption band (see the blue curves in Fig. 3c). The triplet state of Q (^{3}Q*) does not decay during the observation window.

The ^{1}Q* and ^{3}Q* population kinetics are extracted by averaging over their respective bands at 650–1100 nm and 475–580 nm (Fig. 5a). Because of substantial overlap between their spectra, only portions of their bands are averaged to obtain their kinetics. This still captures their true population dynamics because no significant changes in their lineshapes are observed. The kinetics cannot be described as a single unimolecular singlet→triplet intersystem crossing reaction as previously reported for chloranil,[22] but instead require a more complicated reaction scheme like those reported for other ketones.[23, 24] The triplet growth kinetics are often described using a sequential kinetic model, in which the initial ^{1}nπ* state rapidly intersystem crosses in about 1 ps to form the ^{3}ππ* state, followed by a slower internal conversion step to produce the ^{3}nπ* state in about 10 ps. When exciting to the ^{1}ππ* state, a branched kinetic scheme is sometimes invoked,[23] in which the ^{1}ππ* state is able to undergo either intersystem crossing to the ^{3}nπ* state or internal conversion to the ^{1}nπ* state.

Because the ^{1}nπ* state is observed as early as 500 fs for Q (Fig. 3c and Fig. S15), the sequential model more accurately describes intersystem crossing in Q. Using the sequential kinetic model, target analysis was performed on the transient absorption spectrum of Q monomers in cyclohexane (Fig. S8). The formation of ^{3}Q* is described by the time constants of 3.8 ps

and 7.7 ps. The latter value agrees well with the 8 ps triplet formation time constant reported for chloranil in dichloromethane.[22]

4.4. Excited state dynamics of Q:C heterodimers

Over a few picoseconds, the 0.5 ps spectrum of the Q:C heterodimer in Fig. 3d, which resembles that of the Q monomer, decays to reveal ^{3}Q* absorption around 533 nm and an additional peak around 710 nm (green trace, Fig. 3d). Over time, the ^{3}Q* peak decays completely, while the 710 nm band increases in intensity and the sharp 370 nm feature is revealed (see 2000 ps trace in Fig. 3d). The spectrum at 2000 ps matches that expected for the 3,5-di-*t*-butyl-substituted neutral semiquinone (SQ) radical.[12, 25, 26] Although it is difficult to use the visible band to distinguish the neutral and anionic forms of the SQ radical, the 370 nm band is a clear signature of the neutral form; the anionic form contains a distinct peak at 350 nm,[25] which is absent from our spectrum at all times. Therefore, we conclude that neutral SQ radicals are produced in Q:C heterodimers upon excitation at 395 nm via a net hydrogen atom transfer (HAT) reaction from C to Q. Considering that the ^{3}Q* signal of the heterodimer sample in Fig. 5b completely decays by 2 ns due to the formation of SQ radicals, we conclude that the ^{3}Q* state mediates a HAT reaction from C. Note that the complete decay of the ^{3}Q* state in the heterodimer rules out the possibility that the heterodimer dissociates following photoexcitation. If dissociation were to occur, then the long-lived ^{3}Q* state should persist as seen for the Q monomer (blue trace in Fig. 5a).

The 0.5 ps spectrum of Q:C heterodimers in Fig. 3d does not completely match the spectrum of the ^{1}Q* state in Fig. 3c, so we investigated whether additional absorbing species are present. We considered whether the intermolecular hydrogen bond between C and Q could perturb the ^{1}Q* state, giving rise to a redshifted and broadened spectrum. This effect would be similar to the solvatochromic shifts observed for the ground state absorption spectrum of Q in Fig. S5. To test this, the transient absorption spectrum of Q was measured in 2-propanol (Fig. 4a), which is a solvent expected to hydrogen bond to Q and that redshifts the n→π* band of Q to the same location in the Q:C heterodimer (Fig. S4). The ^{1}Q* spectrum averaged between 300 and 700 ps qualitatively matches that of Q in cyclohexane, indicating that excited state hydrogen bonding alone does not produce the 300–700 ps spectrum seen in the Q:C heterodimer and that additional absorbing species are present.

The prominent absorption band at 710 nm in the green trace in Fig. 3d reveals that a neutral SQ radical species is present as early as 10 ps. At this time, the triplet population is not yet quenched, indicating that SQ radicals are also formed from ^{1}Q* states. As such, both singlet- and triplet-mediated HAT reactions are incorporated into a target model used to describe the Q:C heterodimer spectrum in Fig. 3d (Scheme 2a and Fig. S14a). In the target model, it was necessary to include two separate SQ radical states to capture the dynamic narrowing of the 710 nm band seen in Fig. 4c, which we will return to

later. Fig. 4b shows the decomposition of the Q:C heterodimer spectrum averaged between 300 and 700 fs in terms of the SADS from the target model, confirming that there are significant contributions from both the ^{1}Q* and SQ states at this time.

We now consider the bifurcation of the excited state deactivation of ^{1}Q* between the intersystem crossing and HAT channels. From previous work on benzophenone,[21, 24] we expect the hydrogen bonded and non-hydrogen bonded Q molecules to absorb closer to the lower-energy and higher-energy edge, respectively, of the π→π* band. Consequently, the 395 nm excitation likely produces three excited state populations in the Q+C solution: The first (trivial case) is a population of Q* monomers that is accounted for as discussed above. The second is a population of Q:C heterodimers in which the ^{1}Q* molecule is hydrogen bonded with a C molecule at the instant of excitation. The third is a population of Q:C heterodimers in which the hydrogen bond between Q* and C is broken at the instant of excitation. Hydrogen bonding is known to influence electronic excited state dynamics.[27] For example, Venkatraman et al. have reported recently how hydrogen bonding slows down the rate of ultrafast intersystem crossing in benzophenone due to excited state solvation effects.[24] Consequently, the binary distribution of hydrogen bonded and non-hydrogen bonded populations of ^{1}Q* in Q:C heterodimers could be responsible for the bifurcation of its excited state deactivation.

The hydrogen bond lifetime of the Q:C heterodimer is expected to be at least several picoseconds based on MD simulation estimates for benzophenone in methanol and ethanol by Ravi Kumar et al.[21] The expected hydrogen bond lifetime is longer than the longest ^{1}Q* decay time constant, which is 3.8 ps and 3.9 ps in Q monomers and Q:C heterodimers, respectively (Fig. S8 and Fig. S14). We therefore propose that the dynamic hydrogen bond between Q and C in the ground state gates the excited state dynamics. In other words, ^{1}Q* molecules that are not hydrogen bonded with C at the instant of photoexcitation undergo intersystem crossing, while those engaged in a hydrogen bond induce HAT to form the SQ singlet RP state. This is illustrated in Scheme 2a.

The SQ radical formation reaction by ^{1}Q* takes place approximately 1000 times faster than by ^{3}Q* (Scheme 2a). Such a difference between singlet and triplet reactivity of Q highlights the general importance of its complexation to C for enhancing the SQ radical formation efficiency. Nau et al. similarly reported a significantly enhanced hydrogen abstraction reactivity, yet lower efficiency, for bimolecular reactions of excited singlet states of acetone with several different hydrogen bond donors.[28]

We now discuss the necessity of using two states in our target model to describe the SQ radicals formed by photoexcitation of the Q:C heterodimers (Scheme 2a). The dynamic peak narrowing of the SQ band in Fig. 4c, which is reflected by the difference in peak width of the two SADS describing the SQ radicals in Fig. 4d, indicates that their electronic states are perturbed at early time. It is likely that this perturbation results from the electronic coupling[29] between the two proximal SQ radicals that are formed from the Q:C heterodimer. As such, the SADS 2 is assigned to a contact SQ radical pair state, {SQ,SQ},

and the SADS 4 is assigned to a solvent-separated SQ radical pair state, SQ+SQ. In accordance with the target model in Scheme 2a, the contact SQ pairs undergo diffusional separation with a time constant of 14 ps. Such spectral changes from diffusional separation of the SQ radical pairs are reminiscent of the observations made for correlated triplet pair states occurring in molecular films of singlet fission materials, in which the vibronic peak intensity ratios of $T_1 \rightarrow T_n$ PIA bands were found to be sensitive to whether or not the correlated triplet pairs are spatially separated, due to changes in excitonic coupling.[30]

Radical recombination of the contact SQ pairs in the Q:C heterodimers by back HAT is not observed. In particular, the kinetic signal averaged over the 710 nm band (pink data in Fig. 5b) does not decay during the tens of picoseconds timescale. In addition, the GSB signal does not decay toward zero at any time (purple data in Fig. 5c). Note that the rise of the GSB signal does overlap with positive transient absorption features; the early growth of the GSB signal is likely associated with the decay of the overlapping ^{1}Q* peak, and the continued growth of the GSB signal following 200 ps is likely associated with the decay of the overlapping ^{3}Q* peak. Instead of restoring the ground state, the contact SQ pairs separate diffusionally, causing the dynamic narrowing of the SQ band in Fig. 4c. The recombination of the contact SQ pairs would require a HAT event from one SQ to the other. While such a disproportionation reaction is quite efficient for semiquinones in general,[31-34] we propose that it is less efficient for the SQs in this study. Because the intramolecular hydrogen bond in an ortho-semiquinone is twice as strong as in catechol,[31, 35, 36] it stabilizes the radical photoproduct. Additionally, if the intramolecular hydrogen bond in SQ is favored over an intermolecular hydrogen bond between two SQs, the diffusional separation of the contact pair may be facilitated.

5. Conclusions

An o-quinone:catechol heterodimer was used as a model system for investigating how the intermolecular hydrogen bond between quinone- and catechol-containing indolic units in eumelanin may influence its photochemistry. Excitation of the quinone using 395 nm generates singlet excited states that are capable of inducing ultrafast hydrogen atom transfer from the catechol. Some of this population instead undergoes ultrafast intersystem crossing to form triplet states that induce hydrogen atom transfer on a late picosecond timescale. The resulting semiquinone neutral radical pair photoproducts do not recombine during the full time range (2.5 ns) of these measurements. Furthermore, we propose that the dynamic hydrogen bond between Q and C controls the bifurcated deactivation of the singlet excitations.

The results of our model system study show how the specificity of the interfaces between intermolecular hydrogen-bonded indolic units in eumelanin may control their photochemistry. In particular, the *o*-quinone species are capable of inducing excited state hydrogen atom transfer with catechol groups when they are hydrogen bonded, leading to long-lived

semiquinone radical pairs. The chemical heterogeneity proposed for eumelanin[1, 37, 38] intrinsically sets up a wide distribution of intermolecular interactions between indolic units with different redox states. Our study reveals that the hydrogen bonded quinone-catechol interaction sets up a photoinduced hydrogen atom transfer interface that can serve as an ultrafast radical generation center in eumelanin, acting as a source for SQ radicals. Therefore, radical formation may be facilitated in eumelanin structures that are rich in units containing the UVA- and visible-absorbing *o*-quinone functional group. Note that our measurements do not reveal the timescale during which the SQ radicals disproportionate. However, nanosecond transient absorption measurements by Van Anh et al. of both a Q+C mixture and a covalently-tethered Q:C compound reveal long-lived SQ radicals with half-lives of approximately 10 μs and 300 ns, respectively.[12] Therefore, neutral SQ radicals generated at hydrogen-bonded Q:C interfaces are expected to have sufficient time to undergo further radical chemistry. Our study presents a possible photoinduced radical generation pathway in eumelanin that aligns with proposals[39-41] that eumelanin is not only photoprotective, but also a harmful radical source.

Conflicts of Interest

There are no conflicts of interest to declare.

Acknowledgements

This work was supported in part by startup funding from The Ohio State University. The broadband femtosecond transient absorption spectrometer was constructed with partial support from NSF grant CHE-1800471.

References

1. P. Meredith and T. Sarna, *Pigment Cell Res.*, 2006, **19**, 572-594.
2. M. d'Ischia, K. Wakamatsu, A. Napolitano, S. Briganti, J. C. Garcia-Borron, D. Kovacs, P. Meredith, A. Pezzella, M. Picardo, T. Sarna, J. D. Simon and S. Ito, *Pigment Cell Melanoma Res.*, 2013, **26**, 616-633.

3. A. Corani, A. Pezzella, T. Pascher, T. Gustavsson, D. Markovitsi, A. Huijser, M. d'Ischia and V. Sundstrom, *J. Phys. Chem. Lett.*, 2013, **4**, 1383-1388.
4. A. Corani, A. Huijser, T. Gustavsson, D. Markovitsi, P. A. Malmqvist, A. Pezzella, M. d'Ischia and V. Sundstrom, *J. Am. Chem. Soc.*, 2014, **136**, 11626-11635.
5. M. Gauden, A. Pezzella, L. Panzella, A. Napolitano, M. d'Ischia and V. Sundstrom, *J. Phys. Chem. B*, 2009, **113**, 12575-12580.
6. A. Huijser, A. Pezzella, J. K. Hannestad, L. Panzella, A. Napolitano, M. d'Ischia and V. Sundstrom, *Chemphyschem*, 2010, **11**, 2424-2431.
7. J. J. Nogueira, A. Corani, A. El Nahhas, A. Pezzella, M. d'Ischia, L. González and V. Sundström, *J. Phys. Chem. Lett.*, 2017, **8**, 1004-1008.
8. C. Grieco, F. R. Kohl, Y. Zhang, S. Natarajan, L. Blancafort and B. Kohler, *Photochem. Photobiol.*, 2018, DOI: 10.1111/php.13035.
9. D. R. Dreyer, D. J. Miller, B. D. Freeman, D. R. Paul and C. W. Bielawski, *Langmuir*, 2012, **28**, 6428-6435.
10. E. D. Głowacki, M. Irimia-Vladu, S. Bauer and N. S. Sariciftci, *J. Mater. Chem. B*, 2013, **1**, 3742.
11. L. Panzella, G. Gentile, G. D'Errico, N. F. Della Vecchia, M. E. Errico, A. Napolitano, C. Carfagna and M. d'Ischia, *Angew. Chem. Int. Ed. Engl.*, 2013, **52**, 12684-12687.
12. N. Van Anh and R. M. Williams, *Photochem. Photobiol. Sci.*, 2012, **11**, 957-961.
13. J. J. Snellenburg, S. P. Laptenok, R. Seger, K. M. Mullen and I. H. M. van Stokkum, *J. Stat. Soft.*, 2012, **49**, 1-22.
14. M. C. Foti, L. R. C. Barclay and K. U. Ingold, *J. Am. Chem. Soc.*, 2002, **124**, 12881-12888.
15. M. A. Varfolomeev, D. I. Abaidullina, A. Z. Gainutdinova and B. N. Solomonov, *Spectrochim. Acta A Mol. Biomol. Spectrosc.*, 2010, **77**, 965-972.
16. B. N. Solomonov, V. B. Novikov, M. A. Varfolomeev and N. M. Mileshko, *J. Phys. Org. Chem.*, 2005, **18**, 49-61.
17. I. Rozas, I. Alkorta and J. Elguero, *J. Phys. Chem. A*, 1998, **102**, 9925-9932.
18. J. W. Sidman, *J. Am. Chem. Soc.*, 1956, **78**, 4567-4572.
19. H. Bettermann and I. Dasting, *Chem. Phys.*, 1995, **196**, 531-541.
20. A. Berger, P. Hertl and A. Rieker, in *The chemistry of quinonoid compounds*, eds. S. Patai and Z. Rappoport, John Wiley & Sons, Chinchester, 1 edn., 1988, vol. 2, ch. 2, pp. 29-86.
21. V. Ravi Kumar, C. Verma and S. Umapathy, *J. Chem. Phys.*, 2016, **144**, 064302.
22. S. M. Hubig, T. M. Bockman and J. K. Kochi, *J. Am. Chem. Soc.*, 1997, **119**, 2926-2935.

23. H. Satzger, B. Schmidt, C. Root, W. Zinth, B. Fierz, F. FKrieger, T. Kiefhaber and P. Gilch, *J. Phys. Chem. A*, 2004, **108**, 10072-10079.
24. R. K. Venkatraman, S. Kayal, A. Barak, A. J. Orr-Ewing and S. Umapathy, *J. Phys. Chem. Lett.*, 2018, **9**, 1642-1648.
25. S. V. Jovanovic, K. Konya and J. C. Scaiano, *Can. J. Chem.-Rev. Can. Chim.*, 1995, **73**, 1803-1810.
26. P. P. Levin, A. B. Belyaev and V. A. Kuzmin, *Bull. Acad. Sci. USSR, Div. Chem. Sci.*, 1987, **36**, 406-408.
27. G. Zhao and K. Han, *Acc. Chem. Res.*, 2012, **45**, 404-413.
28. W. M. Nau, F. L. Cozens and J. C. Scaiano, *J. Am. Chem. Soc.*, 1996, **118**, 2275-2282.
29. I. R. Gould, R. H. Young, R. E. Moody and S. Farid, *J. Phys. Chem.*, 1991, **95**, 2068-2080.
30. R. D. Pensack, E. E. Ostroumov, A. J. Tilley, S. Mazza, C. Grieco, K. J. Thorley, J. B. Asbury, D. S. Seferos, J. E. Anthony and G. D. Scholes, *J. Phys. Chem. Lett.*, 2016, **7**, 2370-2375.
31. J. J. Warren, T. A. Tronic and J. M. Mayer, *Chem. Rev.*, 2010, **110**, 6961-7001.
32. S. K. Wong, W. Sytnyk and J. K. S. Wan, *Can. J. Chem.*, 1972, **50**, 3052-3057.
33. F. G. Bordwell and J. Cheng, *J. Am. Chem. Soc.*, 1991, **113**, 1736-1743.
34. A. E. Alegria, M. Lopez and N. Guevara, *J. Chem. Soc., Faraday Trans.*, 1996, **92**, 4965.
35. H. Korth, M. I. de Heer and P. Mulder, *J. Phys. Chem. A*, 2002, **106**, 8779-8789.
36. J. S. Wright, *J. Am. Chem. Soc.*, 2001, **123**, 1173-1183.
37. M. d'Ischia, A. Napolitano, A. Pezzella, P. Meredith and T. Sarna, *Angew. Chem. Int. Ed. Engl.*, 2009, **48**, 3914-3921.
38. R. Micillo, L. Panzella, M. Iacomino, G. Prampolini, I. Cacelli, A. Ferretti, O. Crescenzi, K. Koike, A. Napolitano and M. d'Ischia, *Sci. Rep.*, 2017, **7**, 41532.
39. F. Solano, *Polym. Int.*, 2016, **65**, 1276-1287.
40. H. Z. Hill, *BioEssays*, 1992, **14**, 49-56.
41. A. B. Mostert, S. B. Rienecker, C. Noble, G. R. Hanson and P. Meredith, *Sci. Adv.*, 2018, **4**, eaaq1293.

Scheme and Figure Captions

Scheme 1: Eumelanin building blocks (DHI and DHICA) along with chemical structures discussed in the text.

Fig. 1 (a) FTIR spectra of equimolar mixtures of Q+C in cyclohexane. The legend lists the initial concentration of C (or Q) added to the solution. The peaks are identified as free OH (f), intramolecularly bonded OH (b), perturbed intramolecularly bonded OH (b'), and heterodimer (D). (b) The IR absorption spectra of the Q:C heterodimer and C and Q monomers in cyclohexane. (c) Structures of C with and without complexation to Q. O-H bonds are labeled by their type of hydrogen bonding interaction. $\varepsilon_{apparent}$ is the apparent molar absorption coefficient, and ε is the molar absorption coefficient.

Fig. 2 (a) UV/Vis spectra for cyclohexane solutions of the Q monomer, C monomer, and Q:C heterodimer. ε is the molar absorption coefficient. (b) Spectral decomposition of an equimolar mixture of Q+C based on the results from FTIR spectroscopy, showing the absorbance contributions of the C monomer, Q monomer, and Q:C heterodimer.

Fig. 3 (a,b) 2D maps of the transient absorption spectrum of (a) Q monomers and (b) Q:C heterodimers in cyclohexane, measured using 395 nm excitation. The black rectangles mask the scatter appearing in the vicinity of the excitation wavelength. (c,d) Transient absorption spectra at select time delays for (c) Q monomers and (d) Q:C heterodimers. The gray traces in (c) and (d) are the inverted absorption spectra of Q monomers and Q:C heterodimers, respectively. The insets in (c) and (d) show the UV portion of the spectra. The vertical lines at 370 nm are included for reference. The energy level diagram shown in (c) includes electronic transitions for Q in cyclohexane as determined from UV/Vis spectroscopy. The red arrow in (d) emphasizes the sharp feature at 370 nm.

Fig. 4 (a) Comparison of the normalized transient absorption spectra of Q monomers in either cyclohexane or 2-propanol with the Q:C heterodimer spectrum averaged from 300 to 700 fs. (b) Decomposed Q:C heterodimer spectrum from (a) using the target analysis results. (c) Normalized transient absorption spectrum of Q:C heterodimers averaged over the indicated time ranges from 10 to 2200 ps. (d) Normalized species associated difference spectra (SADS) for the two semiquinone (SQ) states. The insets of all graphs show the UV portion of the spectra.

Fig. 5 Transient absorption kinetics averaged over the indicated wavelengths for (a) Q monomers and (b) Q:C heterodimers. (c) Ground state bleach (GSB) kinetics averaged between 415 and 425 nm. Solid lines are fits to the data from target analysis as described in the text.

Scheme 2: (a) Excited state decay pathways determined in this study for the Q:C heterodimer excited at 395 nm. Braces indicate contact pairs. The time constants were obtained from target analysis of the transient absorption spectra. (b) Comproportionation reaction by excited state hydrogen atom transfer (HAT) leading to a pair of neutral semiquinone radicals.

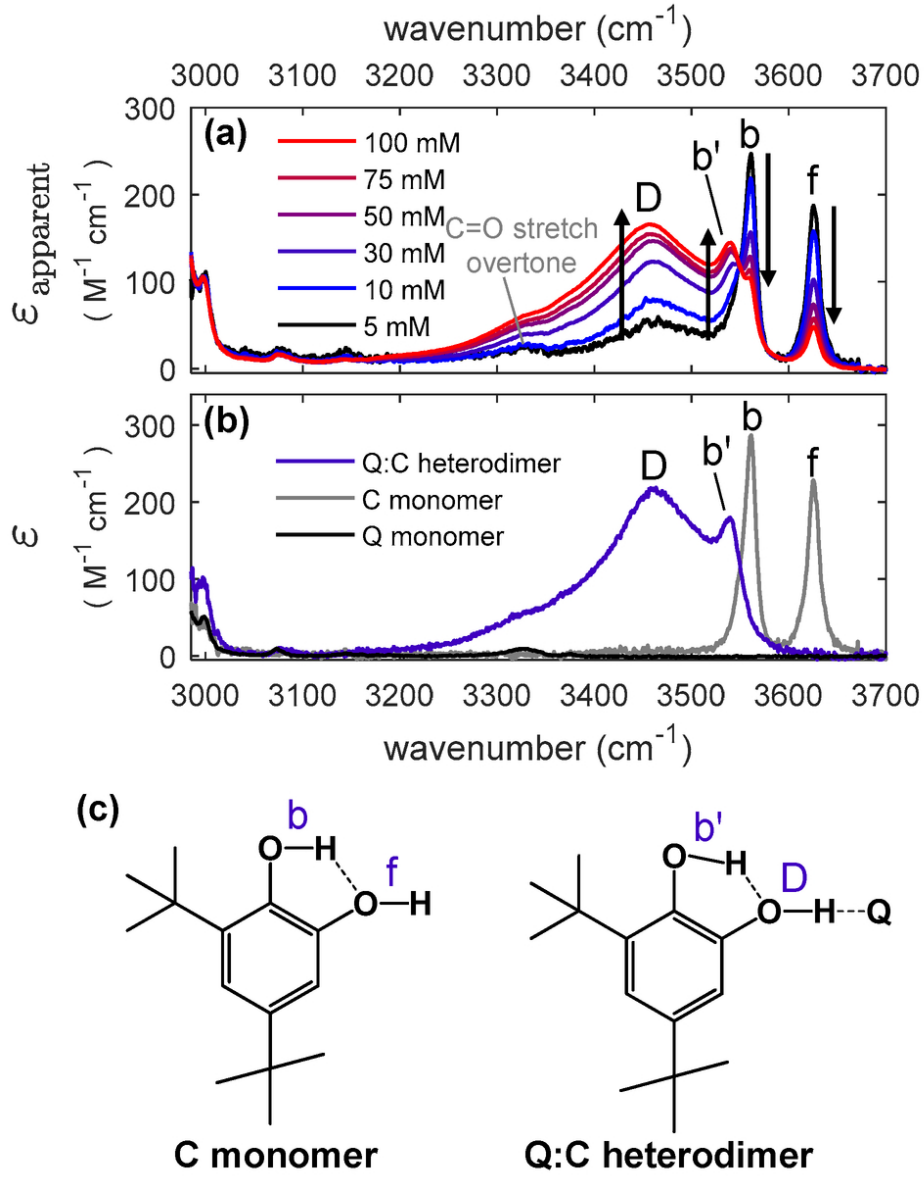

Figure 1

82x103mm (300 x 300 DPI)

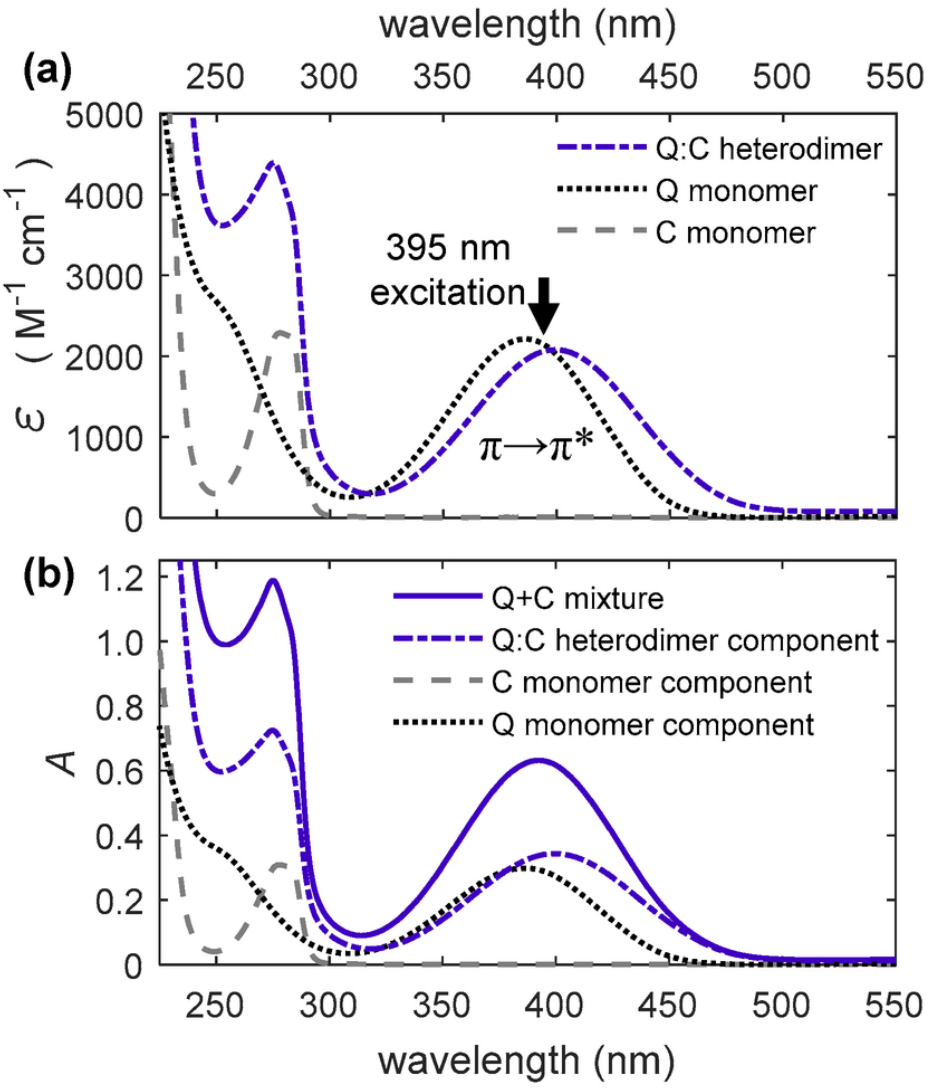

Figure 2

75x83mm (300 x 300 DPI)

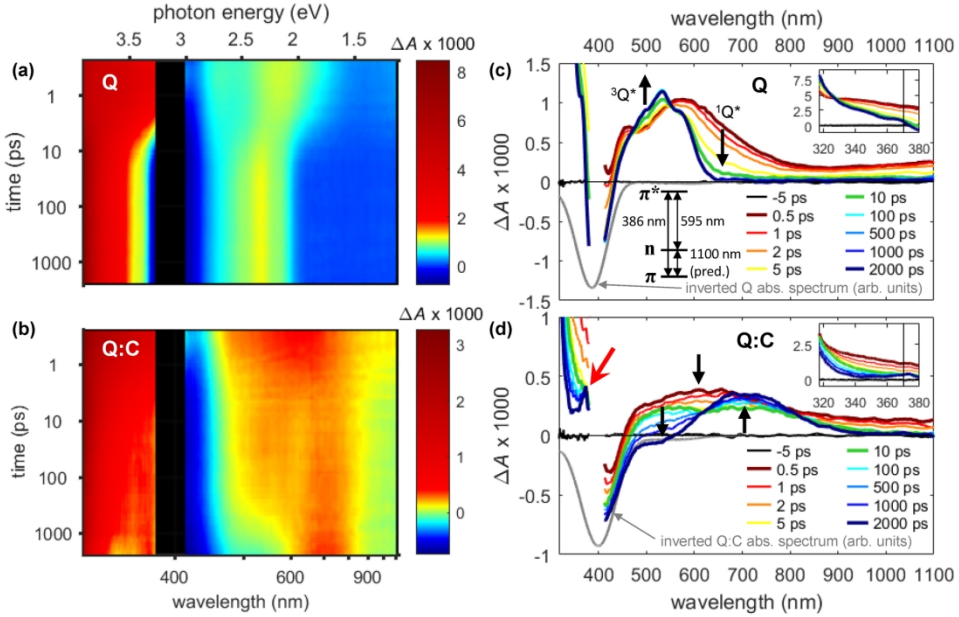

Figure 3

170x107mm (300 x 300 DPI)

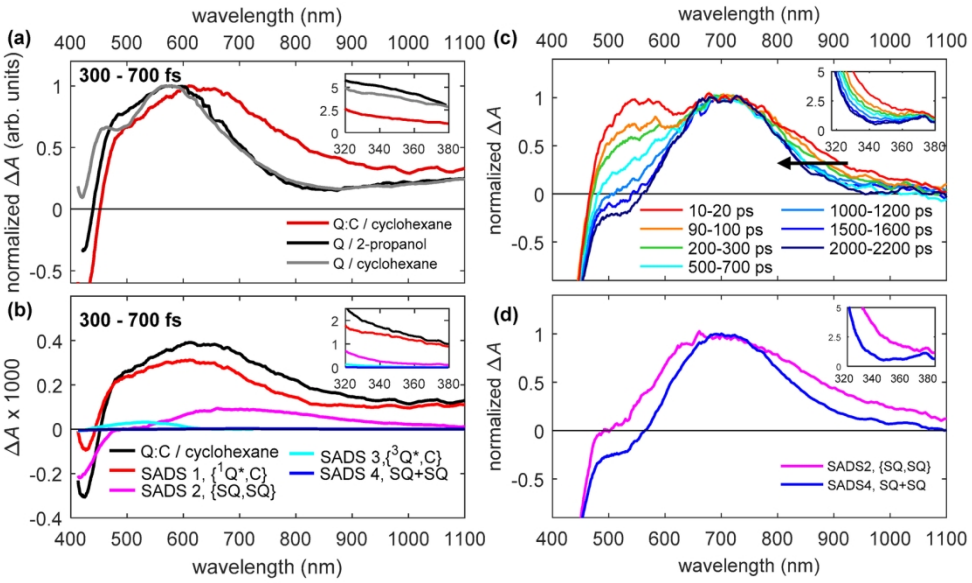

Figure 4

159x93mm (300 x 300 DPI)

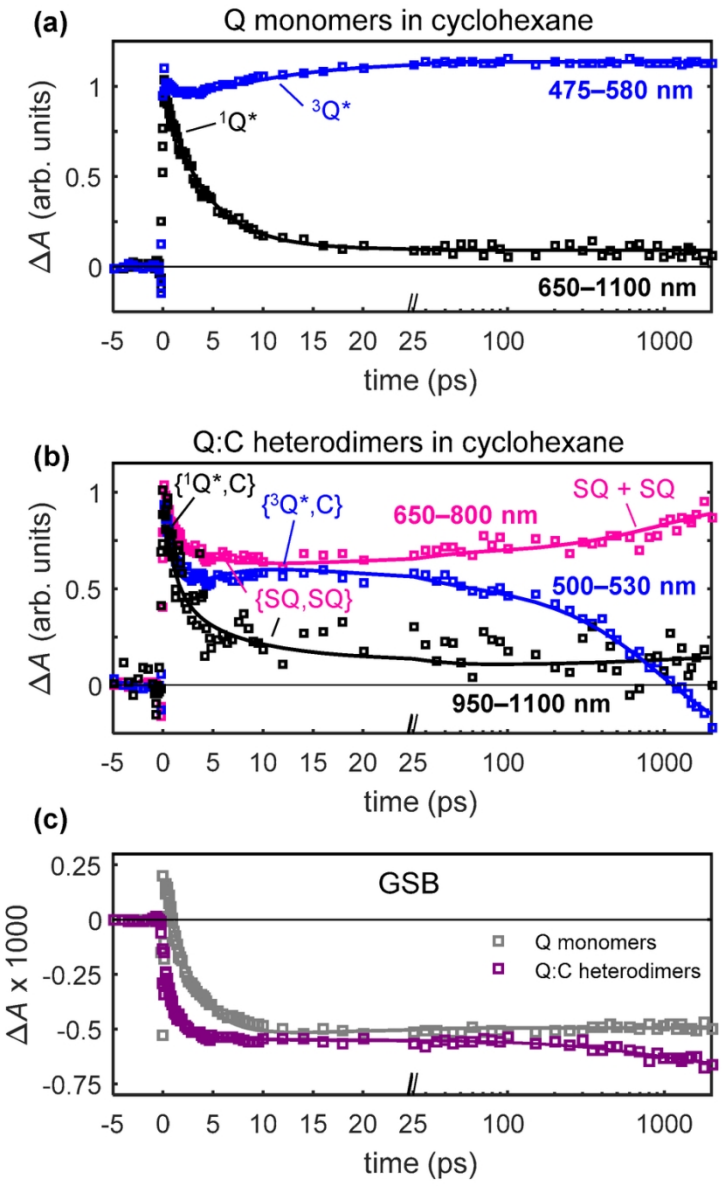

Figure 5

82x132mm (300 x 300 DPI)

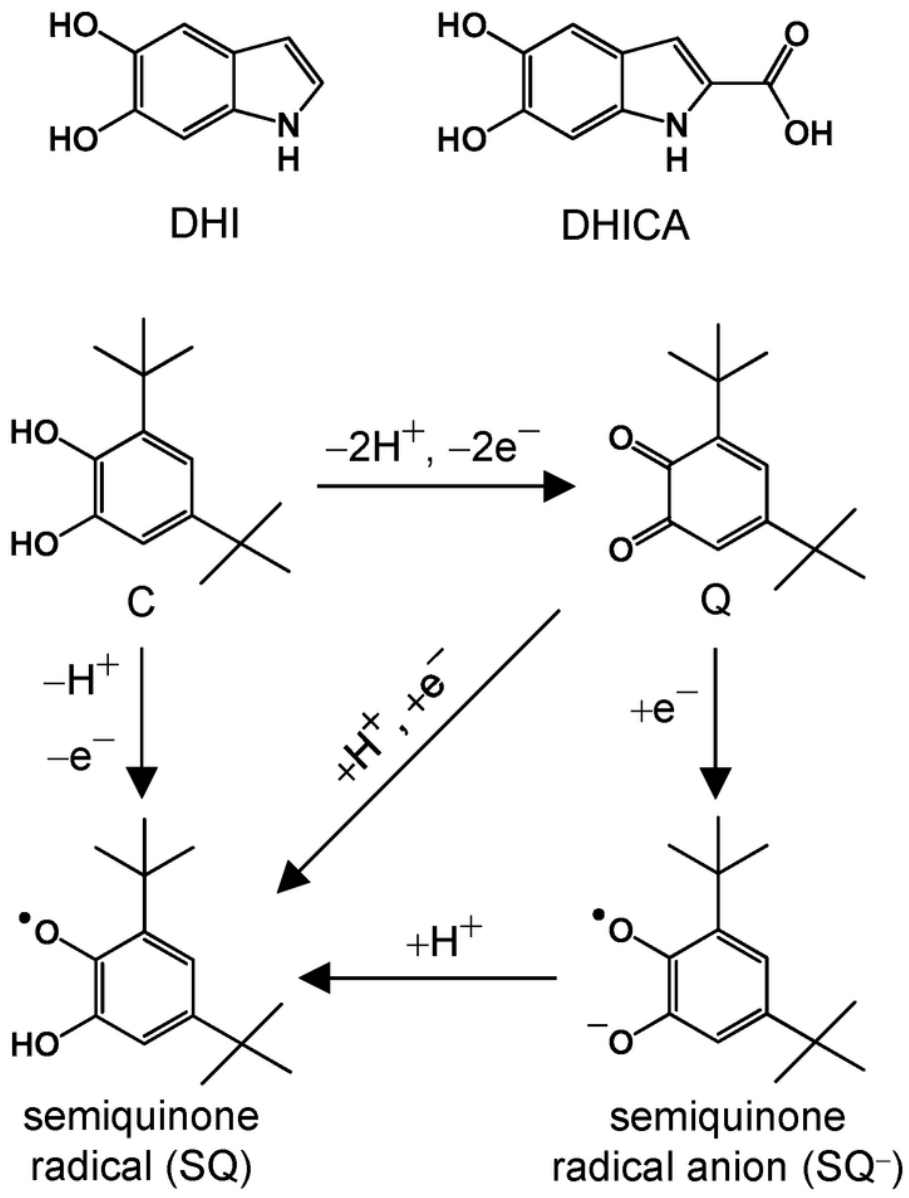

Scheme 1

65x80mm (300 x 300 DPI)

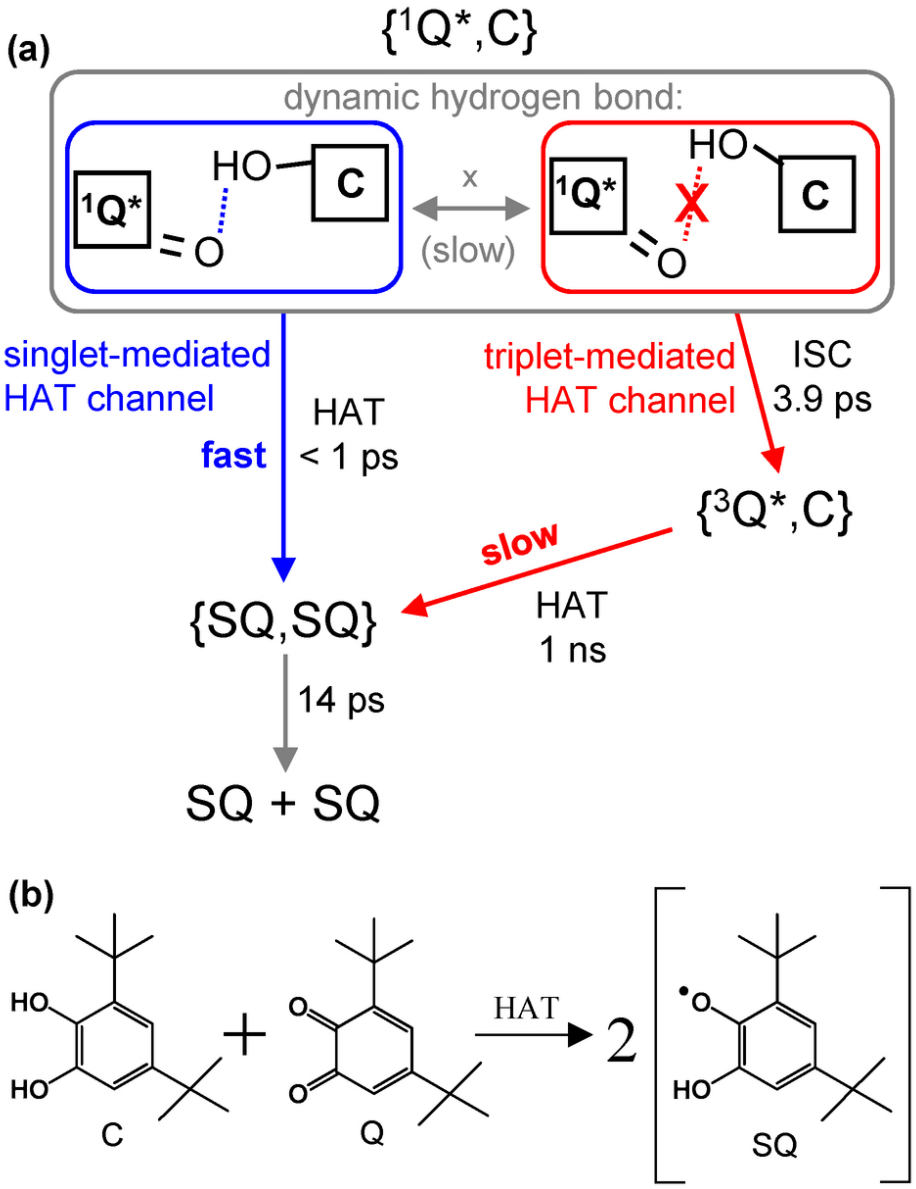

Scheme 2

81x103mm (300 x 300 DPI)

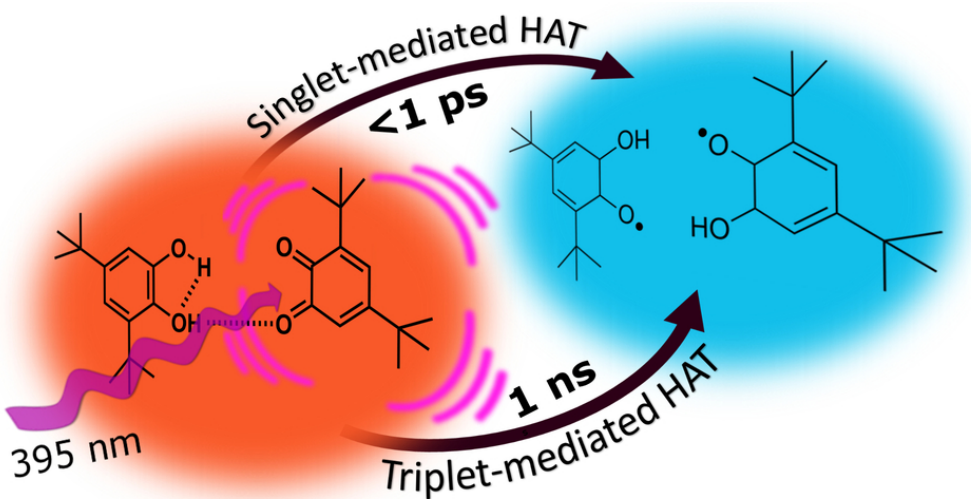

80x39mm (300 x 300 DPI)